



ARL-TR-9360 • DEC 2021



# In-situ Atmospheric Intelligence for Hybrid Power Grids: Volume 3 (Analysis of Whole Sky Image Compression)

by Gail Vaucher, Michael S Lee, and Hailey Goodman

Approved for public release: distribution unlimited.

## **NOTICES**

### **Disclaimers**

The findings in this report are not to be construed as an official Department of the Army position unless so designated by other authorized documents.

Citation of manufacturer's or trade names does not constitute an official endorsement or approval of the use thereof.

Destroy this report when it is no longer needed. Do not return it to the originator.



# **In-situ Atmospheric Intelligence for Hybrid Power Grids: Volume 3 (Analysis of Whole Sky Image Compression)**

**Gail Vaucher and Michael S Lee**

*Computational and Information Sciences Directorate,  
DEVCOM Army Research Laboratory*

**Hailey Goodman**

*Reserve Officers' Training Corps Internship, University of Central Florida*

**REPORT DOCUMENTATION PAGE**

*Form Approved*  
OMB No. 0704-0188

Public reporting burden for this collection of information is estimated to average 1 hour per response, including the time for reviewing instructions, searching existing data sources, gathering and maintaining the data needed, and completing and reviewing the collection information. Send comments regarding this burden estimate or any other aspect of this collection of information, including suggestions for reducing the burden, to Department of Defense, Washington Headquarters Services, Directorate for Information Operations and Reports (0704-0188), 1215 Jefferson Davis Highway, Suite 1204, Arlington, VA 22202-4302. Respondents should be aware that notwithstanding any other provision of law, no person shall be subject to any penalty for failing to comply with a collection of information if it does not display a currently valid OMB control number.

**PLEASE DO NOT RETURN YOUR FORM TO THE ABOVE ADDRESS.**

<b>1. REPORT DATE (DD-MM-YYYY)</b> December 2021		<b>2. REPORT TYPE</b> Technical Report		<b>3. DATES COVERED (From - To)</b> 1 October 2020–30 September 2021	
<b>4. TITLE AND SUBTITLE</b> In-situ Atmospheric Intelligence for Hybrid Power Grids: Volume 3 (Analysis of Whole Sky Image Compression)				<b>5a. CONTRACT NUMBER</b>	
				<b>5b. GRANT NUMBER</b>	
				<b>5c. PROGRAM ELEMENT NUMBER</b>	
<b>6. AUTHOR(S)</b> Gail Vaucher, Michael S Lee, and Hailey Goodman				<b>5d. PROJECT NUMBER</b>	
				<b>5e. TASK NUMBER</b>	
				<b>5f. WORK UNIT NUMBER</b>	
<b>7. PERFORMING ORGANIZATION NAME(S) AND ADDRESS(ES)</b> DEVCOM Army Research Laboratory ATTN: FCDD-RLC-ED White Sands Missile Range, NM 88002-5501				<b>8. PERFORMING ORGANIZATION REPORT NUMBER</b>  ARL-TR-9360	
<b>9. SPONSORING/MONITORING AGENCY NAME(S) AND ADDRESS(ES)</b>				<b>10. SPONSOR/MONITOR'S ACRONYM(S)</b>	
				<b>11. SPONSOR/MONITOR'S REPORT NUMBER(S)</b>	
<b>12. DISTRIBUTION/AVAILABILITY STATEMENT</b> Approved for public release: distribution unlimited.					
<b>13. SUPPLEMENTARY NOTES</b> ORCID ID: Michael S Lee, 0000-0002-0419-6069					
<b>14. ABSTRACT</b> Future Multi-Domain Operation battlefields require uninterrupted electrical power. To enable versatile and resilient resources, the integration and optimization of hybridized power are being investigated. The Atmospheric Intelligence for Hybrid Power Grids (AIHPG) Project is proactively exploiting atmospheric intelligence as part of this effort. One element of atmospheric intelligence comes from whole sky imagers (WSIs). As machine-learning models are applied, the need for additional WSI image data expands, creating a storage space challenge. This report documents research conducted to assess two image compression techniques (image resolution compression [with PNG lossless compression] and image detail compression [using JPEG format]), and three compressed-image applications (peak signal-to-noise ratio, solar radiation diagnostic model, and percent cloud cover assessment). Strengths and weaknesses for these methods and applications are characterized using samples of clear, partly cloudy, and overcast WSI images. The best choice was determined to be a function of the image's application(s).					
<b>15. SUBJECT TERMS</b> image compression, whole sky imager, WSI, hybrid power, atmospheric intelligence, machine learning, peak signal-to-noise ratio, PSNR, solar radiation, percent cloud cover					
<b>16. SECURITY CLASSIFICATION OF:</b>			<b>17. LIMITATION OF ABSTRACT</b>  UU	<b>18. NUMBER OF PAGES</b>  39	<b>19a. NAME OF RESPONSIBLE PERSON</b> Gail Vaucher
<b>a. REPORT</b> Unclassified	<b>b. ABSTRACT</b> Unclassified	<b>c. THIS PAGE</b> Unclassified			<b>19b. TELEPHONE NUMBER (Include area code)</b> (575) 678-2334

## Contents

---

<b>List of Figures</b>	<b>v</b>
<b>List of Tables</b>	<b>v</b>
<b>Acknowledgments</b>	<b>vi</b>
<b>1. Introduction</b>	<b>1</b>
1.1 The Research Problem	1
1.2 Data Resources	2
1.3 Digital Image Analyses	3
1.4 Machine Learning	4
<b>2. Basic Image Compression and Evaluation Tools</b>	<b>5</b>
2.1 Image Resolution Compression	5
2.2 Image Detail Compression	6
2.3 Image Visualization Algorithm for PNG and JPG	7
2.3.1 Clear Sky IRC Example	8
2.3.2 Clear Sky IDC Example	8
2.3.3 Partly Cloudy IRC and IDC Examples	9
2.3.4 Overcast IRC and IDC Examples	11
2.4 Peak Signal to Noise Ratio (PSNR)	12
<b>3. Methods for Testing Image Compression Techniques</b>	<b>12</b>
3.1 Statistical Evaluation: PSNR Evaluation	12
3.2 Diagnostic Model: Solar Radiation	13
3.3 Diagnostic Model: Percent Cloud Cover	14
<b>4. Results</b>	<b>14</b>
4.1 Statistical Evaluation: PSNR Evaluation	14
4.2 File Size versus Compressed Resolutions and Quality Levels	16
4.3 Diagnostic Model Results: Solar Radiation	18

4.4 Diagnostic Model Results: Percent Cloud Cover	20
<b>5. Conclusions</b>	<b>22</b>
<b>6. References</b>	<b>24</b>
<b>Appendix. Maximum File Storage Calculator Program</b>	<b>25</b>
<b>List of Symbols, Abbreviations, and Acronyms</b>	<b>30</b>
<b>Distribution List</b>	<b>31</b>

## List of Figures

---

Fig. 1	Example of a WSI image .....	2
Fig. 2	IRC (PNG) image (2021 March 17, 1400 LT) results at increasing resolutions, followed by the original clear sky image .....	8
Fig. 3	IDC (JPG) image (2021 March 17, 1400 LT) results at increasing QLs, followed by the original clear sky image .....	9
Fig. 4	IRC (PNG) image (2021 March 15, 0910 LT) results at increasing resolutions, followed by the original partly cloudy image .....	10
Fig. 5	IDC (JPG) image (2021 March 15, 0910 LT) results at increasing QLs, followed by the original partly cloudy image .....	10
Fig. 6	IRC (PNG) image (2021 March 16, 0840 LT) results at increasing resolutions, followed by the original overcast image .....	11
Fig. 7	IDC (JPG) image (2021 March 16, 0840 LT) results at increasing QLs, followed by the original overcast image .....	11
Fig. 8	PSNR-IRC (with PNG) experimental data .....	15
Fig. 9	PSNR-IDC (with JPG) experimental data .....	16
Fig. 10	Resolution vs. IRC-PNG file size for each sky condition .....	17
Fig. 11	Quality vs. IDC-JPG file size for each sky condition .....	18
Fig. 12	Predicted vs. actual SR based on TRC-PNG file sizes for a) clear, b) partly cloudy, and c) overcast sky conditions .....	19
Fig. 13	Predicted vs. actual SR based on IDC-JPG file sizes for a) clear, b) partly cloudy, and c) overcast sky conditions .....	19
Fig. 14	Cloud cover chart for PNG file version of test sample .....	20
Fig. 15	File size vs. predicted cloud cover for PNG file type. Ground “truth” value is shown as an orange line. ....	21
Fig. 16	Cloud cover chart for JPG file version of test sample .....	21
Fig. 17	File size vs. PCC for JPG file type .....	22
Fig. A-1	Example of the storage calculator inputs .....	26
Fig. A-2	Example of the storage calculator outputs .....	26

## List of Tables

---

Table 1	Dates, times, and sky conditions of NREL images used for testing .....	3
Table 2	Bit precision and number of colors relationship example .....	4
Table 3	PSNR-IRC (with PNG) results, from processing the WSI images .....	15
Table 4	PSNR-IDC (with JPG) results, from processing the WSI images .....	16

## **Acknowledgments**

---

The authors wish to thank Mr Sean D’Arcy for his work with the Atmospheric Intelligence for Hybrid Power Grids (AIHPG) whole sky imager and the Army Test and Evaluation Command – Meteorology Department (Mr Blaine Thomas) for their field site support with the AIHPG Testbed. Finally, special thanks goes to the Technical Publishing Branch for its technical editing excellence, specifically to Ms Carol Johnson and Jessica Schultheis.

## **1. Introduction**

---

The advancement of digital photography has resulted in a plethora of images, creating a significant and practical challenge regarding how to appropriately preserve the abundance of images without compromising their inherent value. As with any storage issue, the natural response is to remove all unnecessary space within the product. A common method for accomplishing this objective within digital photographs is to use image compression. The success of this method is largely a function of the original image's application. Examples of civilian image applications are safety and/or security surveillance. For such cases, the real-time safety/security images are perpetually acquired and reviewed for content, after which they are archived. In time, however, the ever-growing storage space requirement for the archive becomes overwhelming.

### **1.1 The Research Problem**

---

Future Multi-Domain Operation battlefields require uninterrupted electrical power and, as such, to enable versatile and resilient resources, the integration and optimization of hybridized power are being investigated. The overarching research problem prompting this investigation centered on optimizing isolated hybrid power distribution.

One method for ensuring operational mission effectiveness for an isolated hybrid power grid is to determine and exploit current and future atmospheric conditions. These meteorological conditions are determined using a combination of real-time sky imagery and an atmospheric forecasting model. The results are translated into current and projected power generation potential and then integrated into an energy management system, which determines an optimizing strategy for hybrid power resources. While the meteorological modeling technique and the subsequent power optimization routines are beyond the scope of this report, a practical storage strategy for the sky imagery is the focus of this report.

For this research, the subject images were generated by a whole sky imager (WSI). A sample of the WSI data is shown in Fig. 1. The technology development phase of the parent project, Atmospheric Intelligence for Hybrid Power Grids (AIHPG), required a routine acquisition of real-time WSI images. The image file size was purposefully modest; however, the growing number of image files archived quickly prompted a storage strategy question. With the addition of an advanced machine learning (ML) sky assessment technique that tracks subtle changes over sequential images, the image quality saved took on greater relevance. In the subsequent

sections, WSI data are described, along with their basic formats. A ML overview concludes this introduction.



**Fig. 1** Example of a WSI image

## **1.2 Data Resources**

---

The primary data resource for this study was WSI images from the National Renewable Energy Laboratory (NREL) online database (NREL 2021). The original file format for the 19 selected images was Joint Photographic Experts Group (JPEG or JPG). During the experimentation processes, these photos were re-saved as either a JPG or Portable Networks Graphic (PNG) files, as defined by their research requirement.

WSI images are characterized by their fish-eye, ground-up, sky dome perspective, as seen in Fig. 1. The rectangular digital photographs contain a circular image framed in black. The perimeter of this circle captures an image of the  $360^\circ$  horizontal horizon. The center of the image circle shows the vertical zenith over the photographed site. The images used in this study were sampled during daylight hours with no disc or structure blocking the sun. Note: With specialized photographic sensors, WSI imagery can also be recorded at night.

The NREL images were sampled between 2021 March 15, 0700 MT, and 2021 March 17, 1400 MT, over a NREL site in Colorado. While the sampling rate varied from 10 min to hours, the following captures their general time range by day:

- 2021 March 15, seven images spanned 0700–1420 MT.
- 2021 March 16, five images were acquired between 0630–1010 MT.
- 2021 March 17, seven images ran from 0630–1400 MT.

The images were selected based on a variety of cloud properties, namely, sky type and cloud amounts. Table 1 tallies the WSI image dates, times, and sky conditions used for this project.

**Table 1** Dates, times, and sky conditions of NREL images used for testing

<b>Date</b>	<b>Time</b>	<b>Sky condition</b>
210315	0700	Overcast
210315	0750	Partly cloudy
210315	0910	Partly cloudy
210315	1030	Partly cloudy
210315	1120	Partly cloudy
210315	1230	Partly cloudy
210315	1420	Partly cloudy
210316	0630	Partly cloudy
210316	0800	Partly cloudy
210316	0820	Partly cloudy
210316	0840	Overcast
210316	1010	Overcast
210317	0630	Overcast
210317	0750	Overcast
210317	0950	Overcast
210317	1100	Partly cloudy
210317	1110	Partly cloudy
210317	1310	Partly cloudy
210317	1400	<1/10 (clear)

### **1.3 Digital Image Analyses**

---

Digital camera images were selected for this study. Like humans, digital images are sampled by a sensor (eyes in humans) and interpreted by software (the brain in humans). The human distinguishes color as the amount of light wavelengths reflected onto the retina’s “cone cells”, whereas digital cameras simply capture an image consisting of binary 1’s and 0’s, and need software to interpret the pixels for content and color. For perspective, human image resolution is approximately 576 megapixels, or 18,000 pixels in the vertical direction. These resolutions prohibit humans from seeing a pixelation (Tabora 2019).

In this study, the impacts of image compression were calibrated by using the compressed images to predict solar radiation (SR) as well as discern percent cloud cover (PCC). Differentiating clouds from other image elements required understanding some digital imaging basics. A summary of the key concepts follows.

For the digital camera to record color, the camera uses an array of tiny light-capturing “photosites”. These sensors collect photons from light and store them as quantified electrical signals. A filter is placed on the sensor, which discerns the three primary colors, red, green, blue (RGB), as well as combinations of these colors. In digital imaging, each pixel contains these three channels representing the RGB colors. To recreate the image, an algorithm processes the pixel channels. The image’s bit depth determines the quality of the color information. The more bits stored, the greater the color detail. Table 2 displays a sample of precision and number of colors for each channel type (Tabora 2019).

**Table 2 Bit precision and number of colors relationship example (Tabora 2019)**

<b>Name</b>	<b>Precision (bits)</b>	<b>No. of colors</b>
Monochrome	1	2
Low color	8	256
High color	16	65,536
True color	24	16,277,216

The importance of preserved image details can be seen as one addresses the challenges associated with having the solar disc within the WSI image. The location of the sun within the image has a significant impact on the potential solar energy available for a photovoltaic panel. If the sun is near local zenith, the sun’s rays will have traveled through a minimum number of atmospheres, enabling more energy to reach the surface. In contrast, when the sun rises or sets, the sun’s rays must interact with a significantly larger number of atmospheres, reducing the energy potential. The image colors are also impacted by the longer and shorter sunlight paths. Visually, the net result of a longer sunlight path is often seen as a reddened sky, since the shorter wavelengths (blue) get absorbed by the atmospheric particles encountered along the path; whereas, the longer red wavelengths are able to reach the sensor. When light only has a single atmosphere to traverse, the richness of the blue-sky color can be favorably impacted. Between these two extremes, the variations of blue sky are observed, challenging the RGB ML algorithm’s ability to discern the solar disc, sky objects, and their respective edges.

#### **1.4 Machine Learning**

ML is a form of artificial intelligence capable of learning and improving its performance without being programmed directly, but instead by accessing other computer programs and data resources (Expert.ai 2021). The main goal for ML is to learn without human intervention. This learning technique excels when applied to processing large data quantities that would have otherwise required a significant

amount of human labor hours. As an example, consider web-browser search engines. The search engine not only navigates through a plethora of options, it is also able to use old data from your history to generate new outcomes that are similar to old ones. More examples of ML include fraud detection, spam filtering, malware threat detection, and business process automation (Lee et al. 2018). ML is a crucial and powerful process for many large companies, who use this tool to better understand their customers by processing customer data input, making predictions about what they might search for next. Used in this application, ML allows companies to view and analyze customer trends.

ML can be categorized into four different types: supervised learning, unsupervised learning, semi-supervised learning, and reinforcement learning. In this research, supervised ML (SR Model) was used.

## **2. Basic Image Compression and Evaluation Tools**

---

The primary purpose of image compression is to reduce a file size such that the results can 1) be stored within a particular memory space, 2) potentially produce an improved image file processing rate, 3) enable subsequent applications to fit a smaller analytical processing system, and 4) reduce the number of data set variables—potentially exposing additional data trends or patterns. The challenge is to determine how much compression is appropriate. For this question to be answered, two image compression techniques (image resolution compression [IRC] and image detail compression [IDC]) and three applications (peak signal-to-noise ratio [PSNR], and SR and PCC assessments) were used to determine the best image storage options. An overview of each study component follows.

### **2.1 Image Resolution Compression**

---

IRC reduces the file size by down-sampling and then encoding repeated patterns. Down-sampling—reducing the number of pixels in the width and height of an image—can be achieved many different ways. The simplest approach is called “nearest neighbors”. As an example, to down-sample an image from  $1024 \times 1024$  resolution to  $512 \times 512$  resolution, the neighborhood of  $2 \times 2$  (total of 4) pixels is averaged to yield a single pixel. In this way, the dimensions of the image are reduced in height and width by a factor of 2.

When IRC was executed in the study, the PNG format was used, which further compressed the image without losing any further quality. Lossless compression, such as PNG, searches for repeated patterns to encode and stores the shorthand code with the compressed image. For example, if we use the following sentence as our simulated image, “*The ball bounces up and down, up and down, up and down, etc.*”,

the IRC might take the characters “*up and down*,” and replace them with a “z”, storing this line as “*The ball bounces z z and z etc.*” Thus, saving space. When it comes to reproducing the sentence, the program recalls that  $z = \text{“up and down”}$ , and recreates the sentence in its entirety. Thus, preserving the original document, or image.

In lossless compression, file size reductions are typically no more than 50%–70% of the raw image. Algorithms used for this technique include the Lempel–Ziv–Welch algorithm for pattern matching and encoding, the Huffman coding, arithmetic encoding, and run-length encoding for bit-level packing (Surabhi 2017).

In the case of text-heavy images, PNG methods are preferred over JPG-like methods (described later) for two reasons. First, the sharp discontinuities of text and symbols are easily degraded by the JPG-like methods. Second, the flat gradients of the inner fill of characters and the white spaces between them compress quite well with lossless techniques. Examples of other lossless formats that could be used for IRC are .RAW (often, a propriety camera file format), bitmap (BMP), and Graphics Interchange Format (GIF) (Surabhi 2017; Leonardus 2021).

## **2.2 Image Detail Compression**

---

IDC reduces the image file size by removing details, grouping color and spatial frequencies. This method assumes certain features are irrelevant rather than simply discarding pixels. Algorithms used in this compression method include discrete cosine transforms (DCTs), discrete wavelet transform, fractal compression, and transform encryption. While the image file size can reduce significantly with the general image preserved, there is a significant risk that the image quality will degrade and sometimes require keeping a backup file. Other IDC file traits include the ability to load an application more quickly, and when one zooms in on the compressed image, reaching the pixel level sooner than other formatted images.

The JPG formatted file is an example of an IDC technique. The JPG image file format was designed to yield substantial compression ratios for images by carefully removing information that the human eye is unable to perceive. The encoding process begins with the conversion of the RGB channels to a Y luminance channel with  $C_b$  and  $C_r$  chroma channels. The luminance channel, which is something the eye notices more, is preserved at full resolution, while the two chroma (color) channels are typically down-sampled by a factor of 2 (Wikipedia.org 2021a).

Next, the image is divided into  $16 \times 16$  luminance and  $8 \times 8$  chroma pixel blocks. Each block channel is transformed into spatial frequencies with a type-II DCT. Storage of these transformed blocks is the heart of the JPG compression standard.

Human perception notices large-scale features more than small-scale features. As such, users can select a quality level (QL) from 0 to 100, where a value of 0 provides the most compression and 100 yields the least (but even at the highest QL, some information is still lost). The QL controls how the coefficients of the DCT blocks are quantized into smaller numbers of information bits. For example, a low QL will cause most of the coefficients to be quantized into just a few bits of information. In these cases, only the lowest spatial frequency coefficients will be preserved accurately. Higher QLs will preserve more precision in the middle and higher spatial frequency components. Once QL quantization is completed, a method called Huffman encoding is used to pack the coefficients bit by bit into the encoded JPG file (Wikipedia.org 2021b).

In summary, the QL subdivisions associated with the JPG format signify a range of coefficient weighting used to extract information bits. To delineate this range for this study, a scaling between the 0-quantity level (low QL that preserves less information bits) and the 100-quantity level (high QL maintains more information bits) was referenced in units of percentage (%).

The original JPG standard was defined in the early 1990s and still dominates today, despite several new advancements in image compression technology. JPEG2000 and the intraframe encoder of HEVC/H.265 (Wikipedia.org 2021a) are noteworthy improvements that have yet to achieve universal adoption. In addition, neural networks, with their abundance of nonlinear transformations, hold promise in enhancing image compression even further.

### **2.3 Image Visualization Algorithm for PNG and JPG**

Image visualization scripts were created to better observe the effects of each IRC PNG size (from  $8 \times 8$  through  $1024 \times 1024$ ) and each IDC JPG QL (from 5% to 95%). More specifically, these algorithms were necessary for demonstrating the difference between IRC and IDC. The visualization results were organized in increasing resolutions for the IRC images and increasing QLs for the IDC images. To frame the compression concepts, three sky conditions (representing clear, partly cloudy, and overcast skies) were extracted from the 19-image data set, to demonstrate the effects observed within these multiple PNG resolutions and JPG QLs. Examples of these two key compression techniques are provided in the subsequent sections.

### 2.3.1 Clear Sky IRC Example

The clear sky IRC (with PNG) WSI example shown in Fig. 2 is from 2021 March 17 at 1400 Local Time (LT). The left to right images display nine increasing resolutions, followed by the original image (which is smaller in file size because it was originally a JPG).

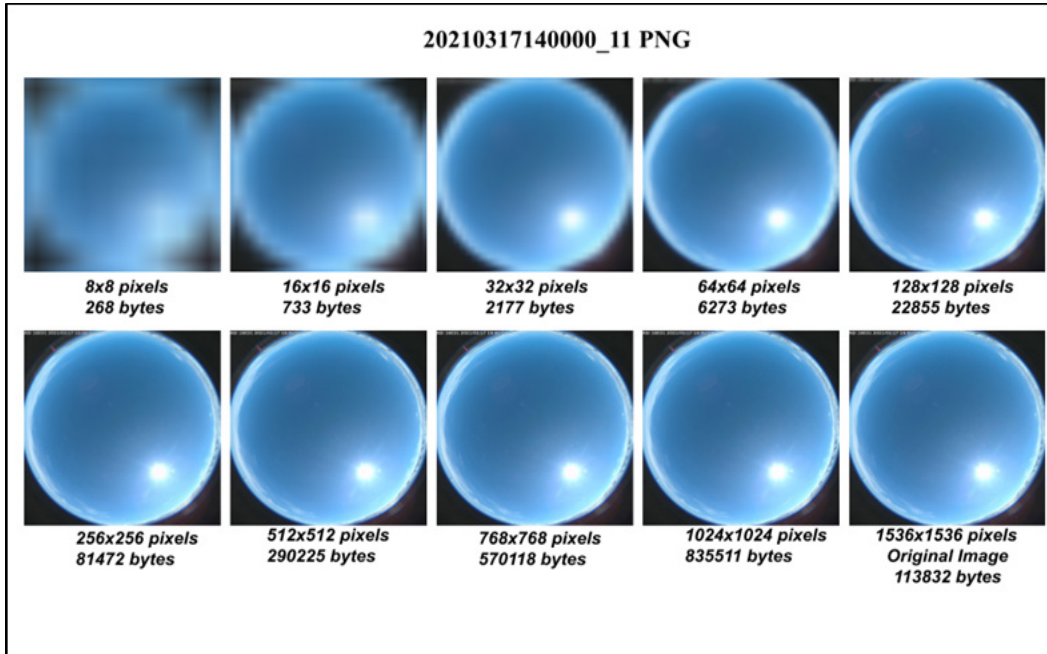
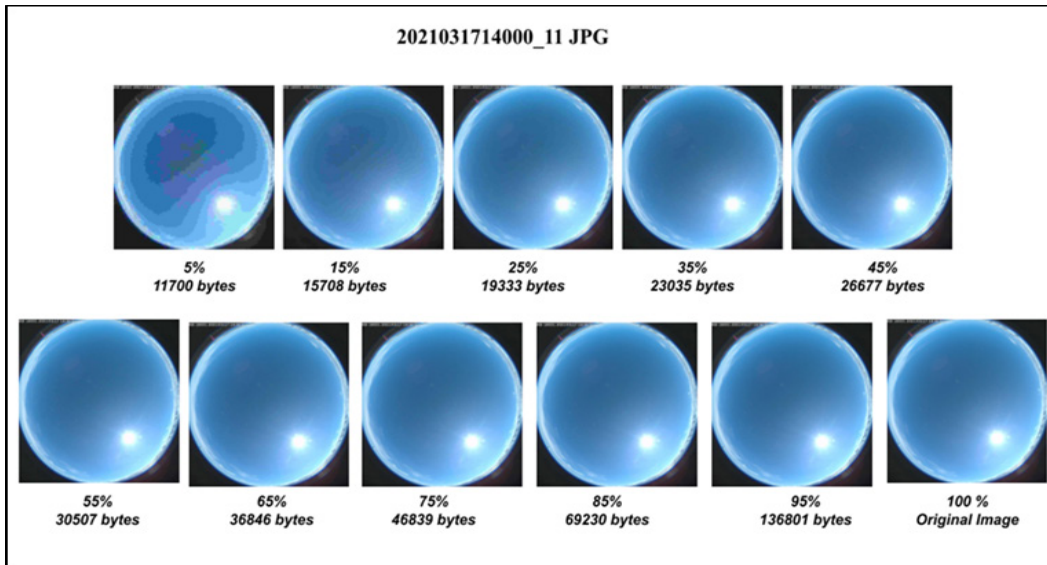


Fig. 2 IRC (PNG) image (2021 March 17, 1400 LT) results at increasing resolutions, followed by the original clear sky image

The IRC loses significant details, as it compresses to smaller file sizes. The  $128 \times 128$  resolution appears to be a threshold between the blurrier  $64 \times 64$  compressed image and the  $256 \times 256$  compression results, which are sharper. Of note, these observations can change depending on how much the images are magnified for viewing.

### 2.3.2 Clear Sky IDC Example

The clear sky IDC (with JPG) WSI example is also from 2021 March 17 at 1400 LT (Fig. 3). The original image (lower right) was IDC-transformed into 10 QL outputs. Figure 3 displays the increase in QL for the clear sky cases (moving left to right, top to bottom).



**Fig. 3** IDC (JPG) image (2021 March 17, 1400 LT) results at increasing QLs, followed by the original clear sky image

The IDC (JPG) compression displays a clear distinction between the color groupings at each QL. At 5%, a broad brush of colors are grouped into a single color, decreasing the file size in the process. As the QL increases, more color detail is preserved. The effects of color grouping is uniquely more evident in the clear sky cases, due to their inherent dynamic range. In terms of balancing visual color details and the associated file reduction, the optimal QL was estimated to be 55% or greater. Additional details for this assessment are discussed later.

### 2.3.3 Partly Cloudy IRC and IDC Examples

A partly cloudy sample from 2021 March 15, 0910 LT, reinforces the IRC and IDC observations, as seen in Figs. 4 and 5.

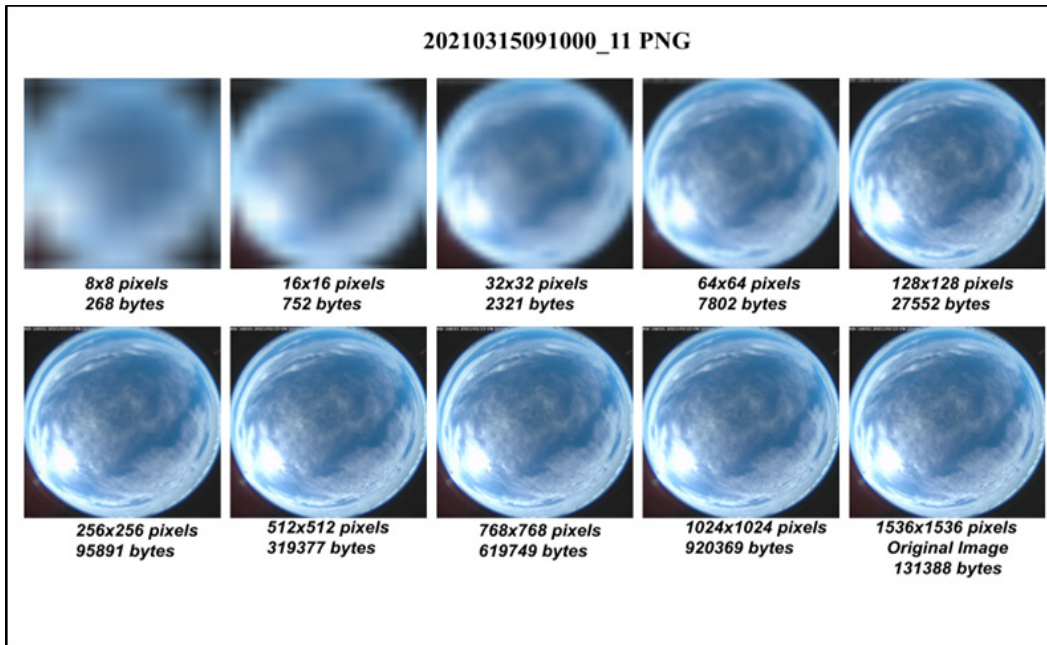


**Fig. 4** IRC (PNG) image (2021 March 15, 0910 LT) results at increasing resolutions, followed by the original partly cloudy image

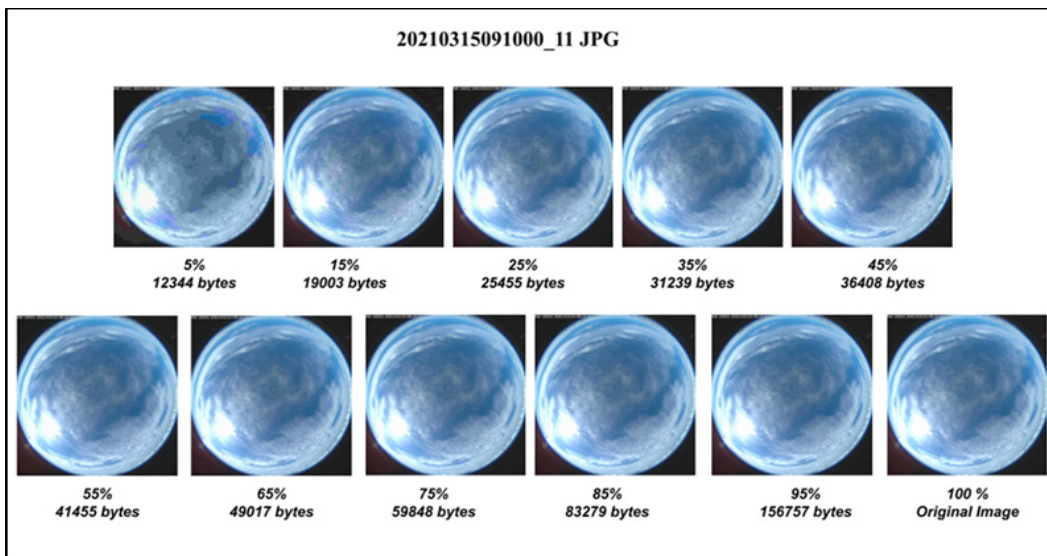


**Fig. 5** IDC (JPG) image (2021 March 15, 0910 LT) results at increasing QLs, followed by the original partly cloudy image

### 2.3.4 Overcast IRC and IDC Examples

Finally, overcast IRC and IDC samples are shown in Figs. 6 and 7.

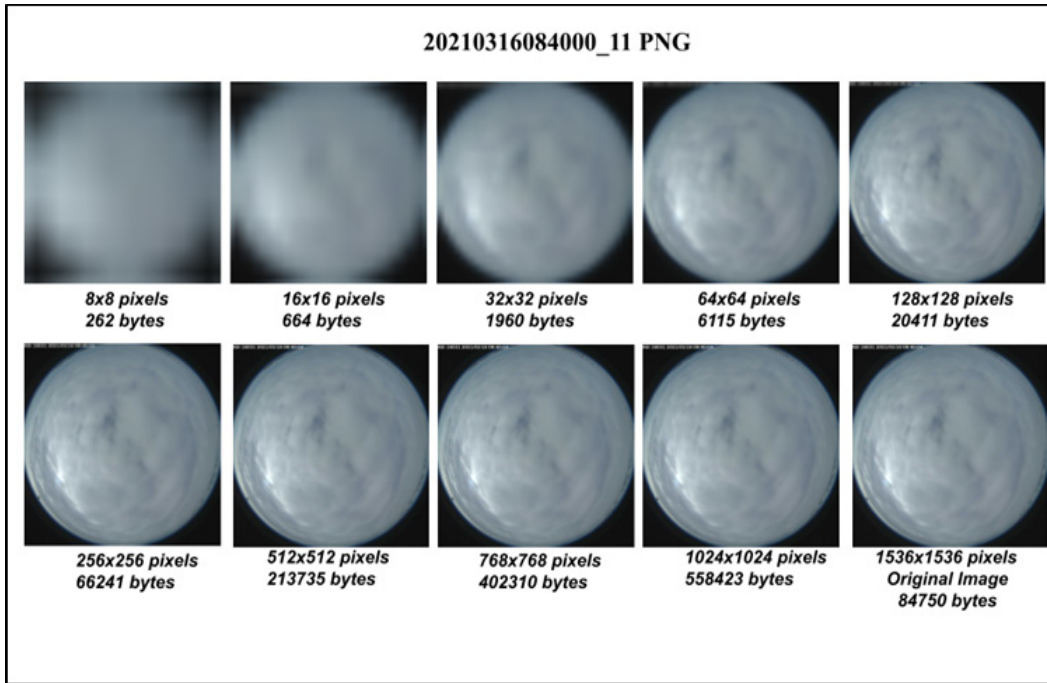


Fig. 6 IRC (PNG) image (2021 March 16, 0840 LT) results at increasing resolutions, followed by the original overcast image

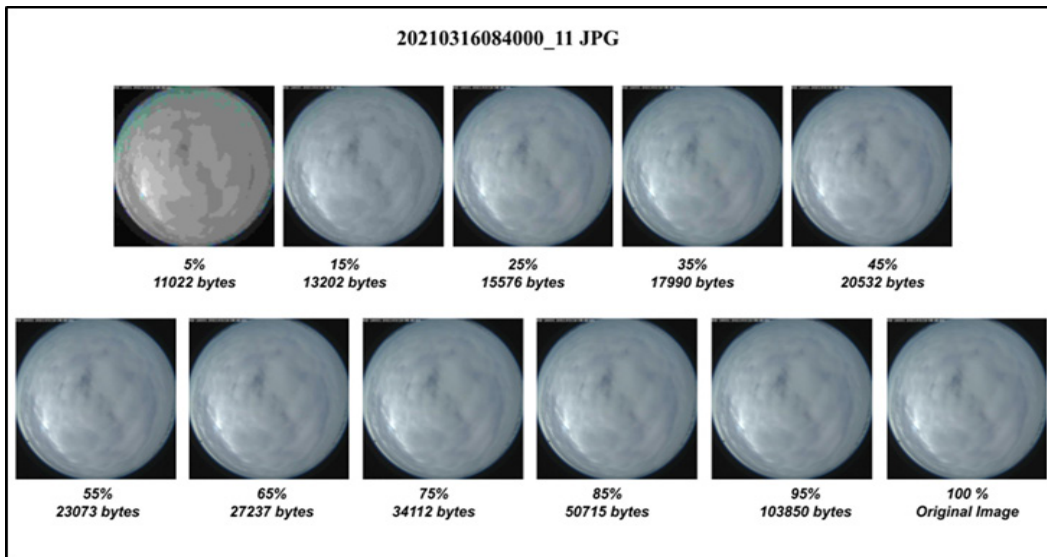


Fig. 7 IDC (JPG) image (2021 March 16, 0840 LT) results at increasing QLs, followed by the original overcast image

## 2.4 Peak Signal to Noise Ratio (PSNR)

---

The metrics used to evaluate image compression were the PSNR and compression ratio (CR). The PSNR represented the pixel error and was expressed as a logarithmic scale in decibels (dB):

$$PSNR = 10 \log_{10} \left( \frac{R^2}{MSE} \right), \quad (1)$$

where  $R$  is the max fluctuation in the input image data type. When  $R$  equals 1, the input image has a double-precision, floating-point data type. For  $R$  equals 255, the image has an 8-bit unsigned integer data type (MathWorks India 2021). The mean-squared error (MSE) captures the discrepancy between the original and compressed image. A smaller MSE indicates a lower error or better match between the initial and compressed images. It follows, then, that a “high” PSNR value indicates a better-compressed image quality (MathWorks India 2021). The PSNR threshold utilized to determine a successful image compression was 35 dB. The best case for an image was defined as having a PSNR above 40 dB (Setiadi 2021).

The CR is defined as the uncompressed file size divided by the compressed file size. As a rule of thumb, to preserve image quality for a JPG, a good CR is 10:1. For the PNG format, the range of CR is generally between 2:1 and 4:1, depending on the image complexity.

## 3. Methods for Testing Image Compression Techniques

---

A quantitative assessment of the image compression techniques was performed using a statistical evaluation, with the PSNR metric as its primary tool. To calibrate the impact of each technique, the compressed images were used as input into two diagnostic models: one that determined SR for the given image and another method that assessed the image’s PCC. Each assessment tool is described next. Their respective results are reported in the subsequent section.

To further address the maximum image storage potential, a maximum storage calculator was independently created and is described in the Appendix.

### 3.1 Statistical Evaluation: PSNR Evaluation

---

The statistical evaluation (a.k.a. PSNR evaluation) used the PSNR parameter as its primary appraisal tool. In this method, the original 19 NREL WSI data images (1536 pixel  $\times$  1536 pixel) were stored in both JPG and PNG formats. Using the PNG format, the following IRC method was executed on the individual images:

- 1) The original ( $1563 \times 1563$ ) individual PNG image was down-sampled (compressed) to one of nine predetermined resolutions ( $8 \times 8$ ,  $16 \times 16$ ,  $32 \times 32$ ,  $64 \times 64$ ,  $128 \times 128$ ,  $256 \times 256$ ,  $512 \times 512$ ,  $768 \times 768$ , and  $1024 \times 1024$  pixels), using a nearest-neighbor technique.
- 2) The compressed image was up-sampled (resized) to the original ( $1536 \times 1536$ ) resolution.
- 3) A PSNR and new file size were calculated and tabulated.
- 4) A copy of the resized image was preserved for further investigation.

The IDC technique processed the JPG images using a slightly different approach:

- 1) The original ( $1563 \times 1563$ ) individual JPG image was down-sampled (compressed) to a fixed resolution of ( $768 \times 768$ ) using the nearest-neighbor technique. This resolution was chosen because it was half the original resolution size, which caused minimal degradation.
- 2) The fixed resolution image was then converted to 10 QLs (5%, 15%, 25%, 35%, 45%, 55%, 65%, 75%, 85%, and 95%) of JPG.
- 3) All 10 of the compressed images were resized back to their original ( $1536 \times 1536$ ) resolution for evaluation.
- 4) A PSNR and JPG file size was calculated for each compressed image at the 10 QLs and tabulated.
- 5) A copy of the resized 10 images were preserved for further investigation.

For results from these two evaluation techniques, see Section 4.

### **3.2 Diagnostic Model: Solar Radiation**

---

A US Army Combat Capabilities Development Command Army Research Laboratory ML model was developed, which used WSI images to determine SR values represented by the photographed whole sky image. To quantitatively assess image compression impact, the 19 test images were grouped into three sky categories: clear, partly cloudy, and overcast. Each image was then subjected to the IRC (PNG) and IDC (JPG) PSNR algorithms. The resulting compressed image was used as input to diagnostic SR model, which determined the image's correlative SR in watts per meters squared ( $\text{W}/\text{m}^2$ ). The comparative SR ground-“truth” values were acquired through the same data resource as the original images. The results are shown in Section 4.

### **3.3 Diagnostic Model: Percent Cloud Cover**

---

The PCC experiment began with a seasoned meteorologist assessing the cloud cover for the test image. Due to research time constraints, only one image (partly cloudy) was tested. The scale for cloud cover percentages ranges from 0% (no clouds) through 100% (overcast). The typical gradient is recorded in tenths; however, for this study, an exception was made, which included defining the test image as between 30% and 40% cloud cover. This numeric assessment [35 ( $\pm 4$ ) %] was independently validated using MATLAB image processing functions. Image analysis Python scripts were created to determine PCC from PNG and JPG WSI images.

Per the earlier IRC process description, the PCC-PNG algorithm down-sampled the single test image into nine resolutions. The image was then up-sampled to the original resolution. The DEVCOM Army Research Laboratory PCC algorithm evaluated cloud cover by analyzing the RGB channel content, replicating the MATLAB functions. The final image, PCC, and file size for each compressed resolution were preserved for review.

The IDC process utilized a fixed resolution for the compression step. The compressed JPG images were up-sampled to the 10 QLs, as defined in an earlier section. Each quality level image was then used as input by the PCC-JPG algorithm. The resulting compressed image, PCCs, and file sizes were preserved for analysis.

The results are presented in Section 4.

## **4. Results**

---

---

The results from the statistical evaluation and each of the two image applications follow. As an auxiliary product to the statistical evaluation, a comparison of file sizes with respect to the 9 resolutions and 10 QLs was conducted. These results are in Section 4.2.

### **4.1 Statistical Evaluation: PSNR Evaluation**

---

A sample of the PSNR evaluation results are graphically displayed in Figs. 8 and 9. These plots represent both the IRC (PNG) and IDC (JPG) image compression techniques. The PSNR threshold of 35 dB is notated by an orange horizontal line. The resulting file sizes (in bytes) are scaled along the x-axis. The visual stacking of data is an interesting artifact of the multiple image cases, as they horizontally sequence through the 8 pixel resolutions (shown) and 10 QLs.

The PSNR-IRC results (Fig. 8) indicate that about half of the compressed images were at or above 35 dB. This favorable product was initially observed once the compressed image had a file size of about 6 MB, as seen in Table 3. The compressed images for the two highest resolutions (512 and 1024) generated PSNR values consistently above 35 dB. This pattern implies that photos with greater image resolutions do not significantly jeopardize the image quality.

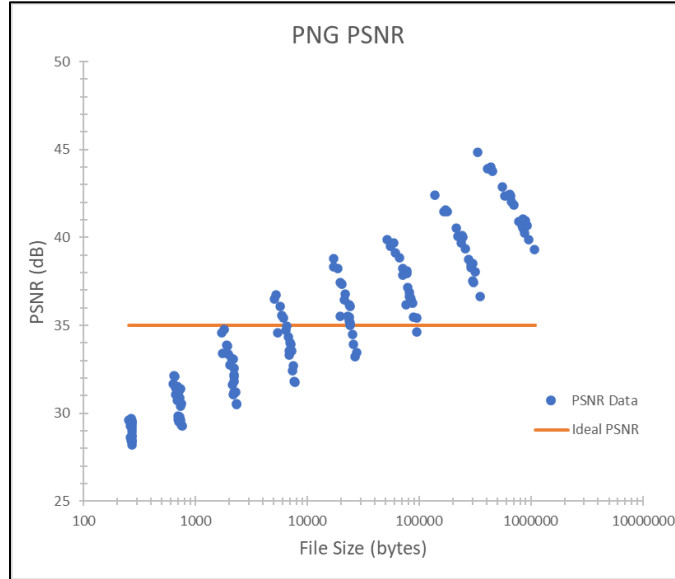


**Fig. 8 PSNR-IRC (with PNG) experimental data**

Table 3 presents a sample of the numerical values used in Fig. 8. The plotted values only include the pixel-doubling counts. The 768-pixel case (not plotted) is tabulated for reference.

**Table 3 PSNR-IRC (with PNG) results, from processing the WSI images**

<b>Resolution (pixels)</b>	<b>File size (bytes)</b>	<b>PSNR (dB)</b>
88	268	29.5
16	686	31.5
32	1,924	33.8
64	5,924	35.6
128	19,554	37.5
256	61,312	39.1
512	171,201	41.6
768	307,980	42.9
1024	436,133	44.0

Figure 9 shows the PSNR-IDC (with JPG) experiment results. Contrasting this figure with Fig. 8, there are more PSNR-IDC (with JPG) results at or above the

35-dB threshold than for PSNR-PNG. Here, the visual alignment is a function of the 10 unique QL delineations (Table 4). Note the consistent increase in both QL and file size.

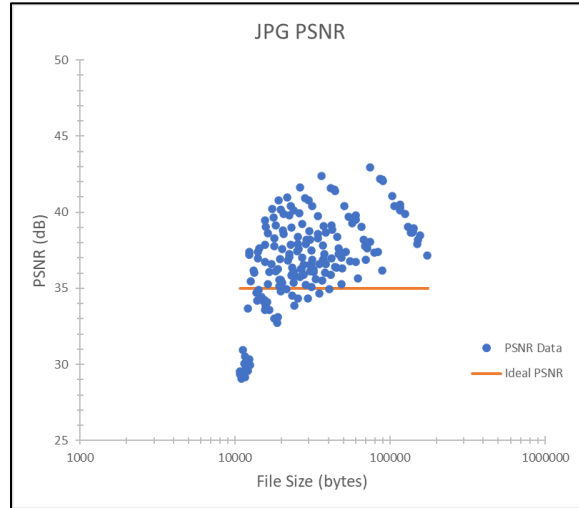


**Fig. 9 PSNR-IDC (with JPG) experimental data**

**Table 4 PSNR-IDC (with JPG) results, from processing the WSI images**

Quality level	File size (bytes)	PSNR (dB)
5	11,036	29.5
15	13,305	36.0
25	15,590	37.9
35	17,900	38.3
45	20,264	38.8
55	22,373	39.8
65	26,052	40.0
75	31,568	40.4
85	44,390	41.4
95	88,818	42.2

While the IDC-JPG results showed greater points above the 35-dB threshold, the size of the “successfully” reduced file starts at slightly over twice the file size of the PNG’s initial favorable results [IDC-JPG (13305 bytes) vs. IRC-PNG (5924 bytes)]. Finally, both IDC and IRC schemes show a pattern whereby larger file sizes are correlated with greater PSNR values.

## **4.2 File Size versus Compressed Resolutions and Quality Levels**

File size is a key parameter in this study; therefore, plots were generated to compare the compressed resolutions and QLs against this variable. To better assess the resulting impacts, the original images were divided into the three sky conditions

(clear, partly cloudy, and overcast). Figure 10 shows the compressed file size versus compressed resolution. For all sky conditions, the file size increased with the image resolution. For almost all cases, the partly cloudy files generated a relatively larger file size than the other sky conditions. Especially at higher resolutions ( $\geq 256$  pixels), the IRC (with PNG) overcast file size was less than the clear and partly cloudy counterparts.

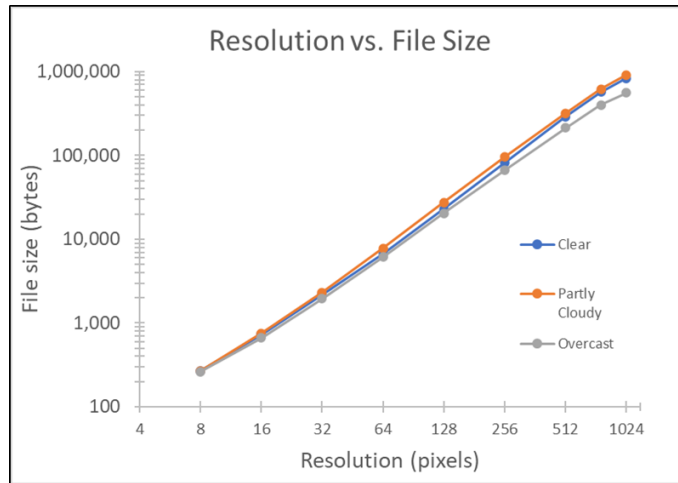


**Fig. 10 Resolution vs. IRC-PNG file size for each sky condition**

Implied in these numbers is the concept that more-complex images yield larger file sizes. One would expect that flat color images like an overcast sky would have the least complexity and therefore the best compression. On the other hand, partly cloudy skies are the most-complex scenes of the three examples, and therefore require larger amounts of information to encode the image accurately.

The relationship between an image's compressed QL and JPG file size is shown in Fig. 11. Here, as the QL increased, the file size did likewise. This rate of change lessened between quality values of 35%–55% and sharply increased between the last two values of 85% and 95%. In all cases, the compressed partly cloudy file size maintained a larger file size than the clear and overcast equivalent files. As is seen later, the partly cloudy files also generated the more accurate SR diagnoses. Overcast cases consistently sported the leanest of the three sky-type file sizes, at each QL.

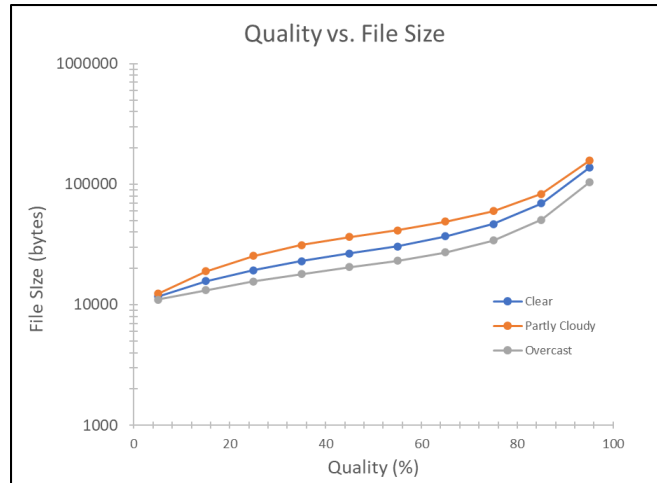


**Fig. 11 Quality vs. IDC-JPG file size for each sky condition**

### 4.3 Diagnostic Model Results: Solar Radiation

The diagnostic SR model experiment results were divided into three sky types (clear, overcast, and partly cloudy) and two image compression schemes (IRC-PNG and IDC-JPG). The targeted ideal was to match the pre-established SR magnitude associated with the original image to the SR generated when using the processed image as input for the ML SR model. A sample of the PNG and JPG case results for all three sky types is shown in Figs. 12 and 13. Note: The orange line shows the actual SR value (“ground truth”) for the given day/time.

For the SR IRC-PNG clear and partly cloudy cases (Fig. 12), the reassessed SR results were significantly closer to the ground truth, as the file size increased (x-axis). In fact, for the partly cloudy cases, the two largest file sizes show the predicted SR value as being met and exceeded. Oddly, the overcast case showed a growing separation of magnitudes as the image dimensions increased from 8 to 512 pixels, followed by a leveling off of values for the remaining four largest file sizes.

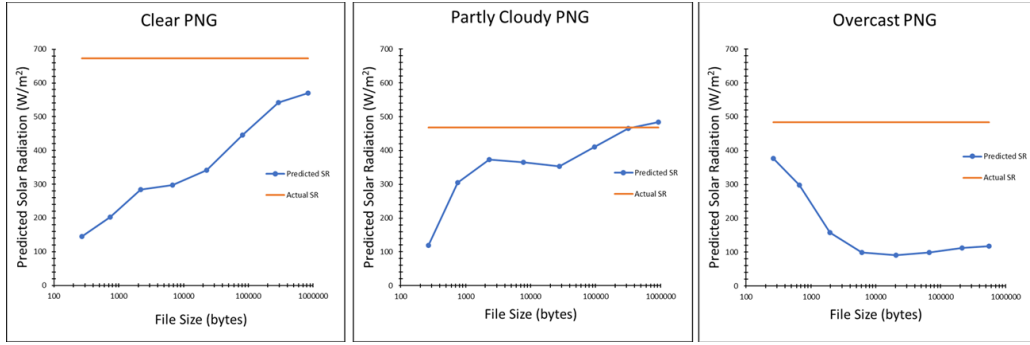


**Fig. 12** Predicted vs. actual SR based on TRC-PNG file sizes for a) clear, b) partly cloudy, and c) overcast sky conditions

The SR-IDC (JPG) cases (Fig. 13) showed a very different response: the initial clear sky case nearly matched ground truth and then plummeted to a level that persisted for almost all larger file sizes. The partly cloudy case started in near unison and then hovered-around ground truth as the file sizes increased. The overcast case consistently, and significantly, underestimated the target value for all file sizes. The relative persistence in overcast case magnitudes is noteworthy.

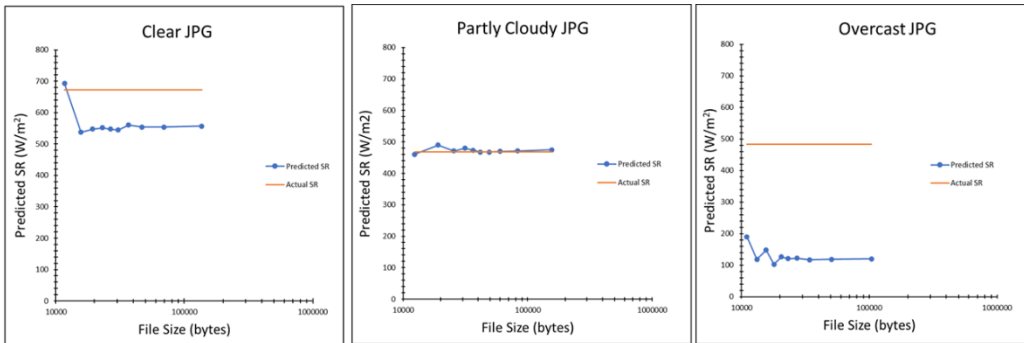


**Fig. 13** Predicted vs. actual SR based on IDC-JPG file sizes for a) clear, b) partly cloudy, and c) overcast sky conditions

Using results from an independent SR sensor comparison (Bergen 2021), an acceptable irradiance value was defined with a bias of 6%. Even with this mean bias error, the accuracy of the predicted SR for both PNG and JPG clear and overcast cases has room for improvement. In terms of operational impact, however, the consistency of the JPG compression results indicates that for this SR model, increasing the compression file size did not significantly affect the SR forecast precision. This IDC-JPG precision trait reflects the IRC-PNG overcast case.

As seen previously, this sky condition also presented results that more closely aligned with ground truth. Perhaps, the added cloud-sky contrasts natural to partly cloudy images, translated into informative image details, which resonated with the ML assessment, even at leaner compression sizes.

Coupling the earlier statistical observation regarding IDC images showing sufficient detail at and after 55% QL, the application of these same images for diagnosing SR, levels off and becomes more precise after 55%. Perhaps this occurs because the image has enough consistent details (e.g., less color grouping) to generate a stable SR value. Though the results are not always accurate, the solution might be improved with a correction factor applied to the clear and overcast image cases.

#### 4.4 Diagnostic Model Results: Percent Cloud Cover

For the PCC diagnostic model test, the PCC ground truth for the given image was evaluated to be 35% ( $\pm 4\%$ ) (see Section 3). Using the IRC and IDC compressed images, a PCC was assessed for each image.

Figure 14 displays the progression of IRC (PNG) resolutions. Image resolution, file size, and the evaluated PCC are listed under each image. As noted earlier, the visual threshold between blurry and relatively clear images is about  $128 \times 128$  pixels.

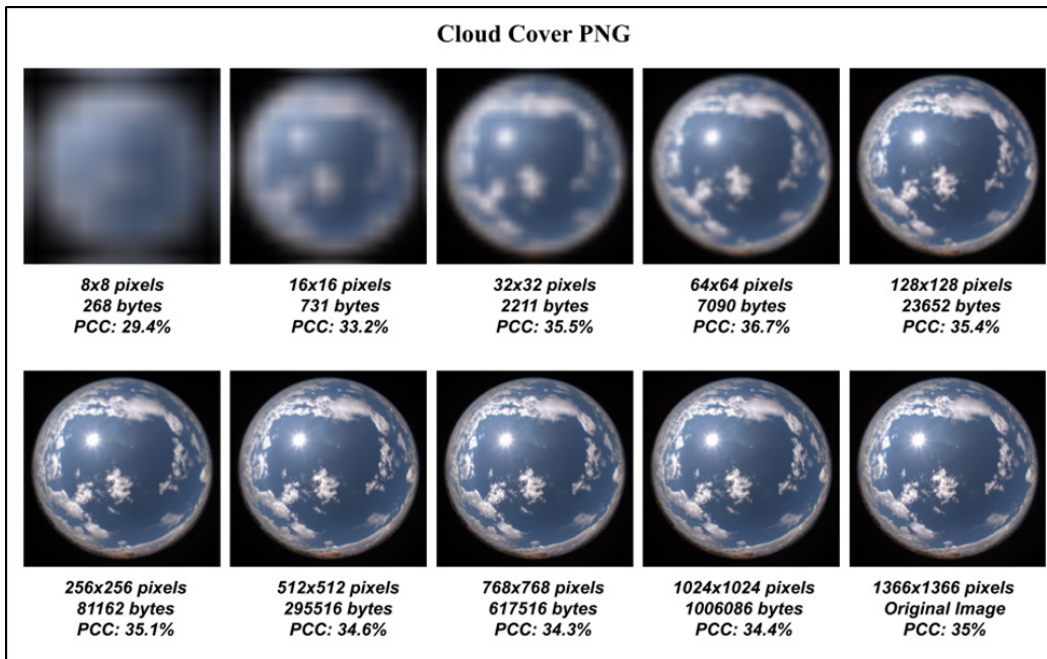
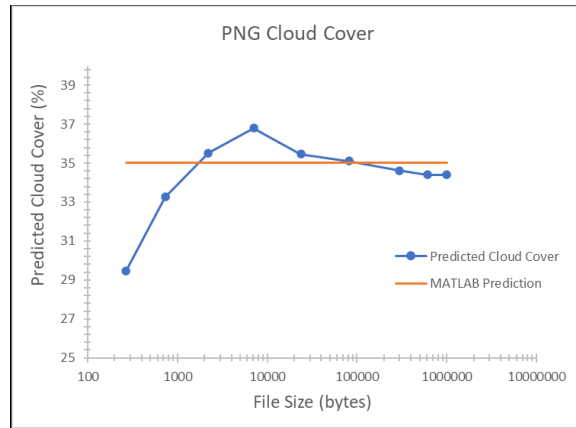


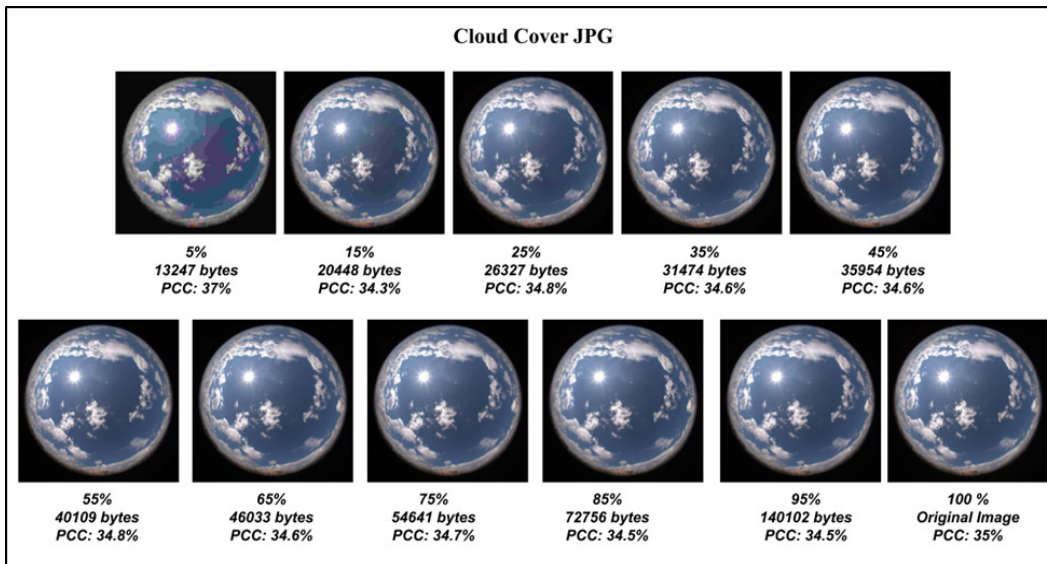
Fig. 14 Cloud cover chart for PNG file version of test sample

Reviewing the results graphically (Fig. 15), the PCC-PNG images produced cloud cover results within the acceptable value for all but the  $8 \times 8$  resolution, which reported a PCC of 29%. This output likely occurred because the extremely reduced file size/resolution did not contain enough detail for the PCC model to determine an accurate result.



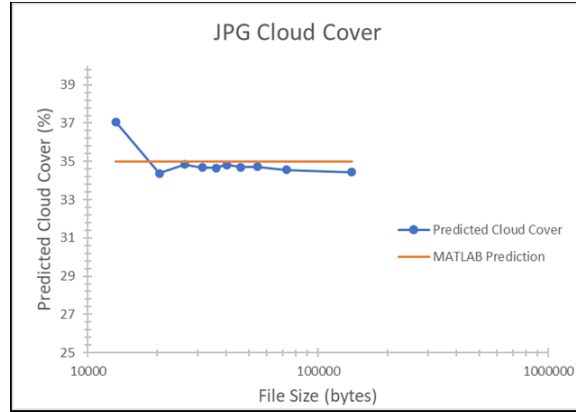
**Fig. 15** File size vs. predicted cloud cover for PNG file type. Ground “truth” value is shown as an orange line.

Figure 16 displays the progression of IDC (JPG) QLs. Under each image is listed the respectively QL, file size, and PCC. Reviewing the results, all levels report acceptable PCC values.



**Fig. 16** Cloud cover chart for JPG file version of test sample

Figure 17 graphically displays the file size versus PCC for the PCC-JPG experiment. Successful PCC values are reported at all QLs. For this case, the IDC compression method reduced files sizes significantly, while maintaining a significant amount of detail for the algorithms to determine an accurate PCC output.



**Fig. 17 File size vs. PCC for JPG file type**

These results align with the three sky classification IDC results, where the partly cloudy case distinguished itself in more accurately calculating SR based on the compressed image. In this PCC experiment, the compressed partly cloudy image may have a relatively larger file size, but above 5% QLs, it also retains enough PCC-relevant details to both accurately and precisely calculate the PCC.

## 5. Conclusions

---

Strengthening the provision of uninterrupted electrical power is being pursued through the exploitation of atmospheric intelligence into hybridized power grids. One element of the atmospheric intelligence comes from WSI images. As ML algorithms are developed to analyze the WSI data, there is an increased need for images to train and test these algorithms. Smartly storing these many images requires planning and strategy. Image compression is a natural approach to this problem.

In this study, the challenge of how to maximize WSI image storage while still enabling the image analysis applications to be satisfied was addressed. Two image compression techniques were investigated: IRC enhanced by the PNG format and IDC executed with the JPG format. For the IRC method, nine resolutions were evaluated. The IDC method compressed images to a fixed resolution, followed by detail recompression at 10 QLs. The resulting image was then compared to the original image and tested.

The evaluation of impact was first quantified by the parameter, PNSR, using a threshold of 35 dB or greater to indicate an acceptable result. Numerically, the IDC (JPG) results showed more value in the accepted category. The IRC (PNG) acceptable values were noted for the upper resolutions.

The processed images were subdivided into three sky conditions (clear, partly cloudy, and overcast) and evaluated as a function of file size. Overcast skies showed the smallest file size for both resolution and QL data results. Partly cloudy showed the greater file size, with clear sky cases drifting between these two sky conditions.

The compressed images were then submitted as input for two diagnostic models: SR and PCC diagnostic assessments. The SR evaluation for the IRC (PNG) images were mixed. Clear and partly cloudy showed improvements, as the PNG file size increased. Overcast had its “best” result with the smallest file size.

The IDC (JPG) SR evaluation reported significant precision (as the file size increased) in the three sky conditions results, with only the partly cloudy case showing accuracy. The accuracy results may have been influenced by the developmental nature of the SR model.

The execution of the PCC experiment was constrained by time, but showed favorable results with its single image test case. Both IRC and IDC showed acceptable results at most resolutions and QLs, respectively. Numerically, the precision of the IDC results (as file size increased) was notable.

Armed with the previous characterization of the compression routine impacts, the strengths and weaknesses of each technique were weighted against mission applications and requirements. In short, the “best choice” was determined to be a function of the image’s current and future application. With these results, an informed decision is now possible.

## 6. References

---

- Cadet Bergen S. ROTC Internship, DEVCOM ARL. Personal communication, 2021 July 30.
- Expert.ai. What is the definition of machine learning? Expert.ai; 2020 May 6 [accessed 2021 May 26]. <https://www.expert.ai/blog/machine-learning-definition/>.
- Lee M, Valisetty R, Breuer A, Kirk K, Panneton B, Brown Scott. Current and future applications of machine learning for the US Army. Army Research Laboratory (US); 2018. Report No.: ARL-TR-8345, <https://apps.dtic.mil/sti/pdfs/AD1050263.pdf>
- Leonardus N. Lossy vs. lossless image compression. Hostinger Tutorials; 2021 Apr 19 [accessed 2021 Nov 1]. <https://www.hostinger.com/tutorials/lossy-vs-lossless>.
- National Renewable Energy Laboratory. Measurement and Data Instrument Center MDIC. Department of Energy (US); n.d. [accessed 2021 Mar]. <https://midcdmz.nrel.gov/apps/sitehome.pl?site=SRRLASI>.  
*Any publication based in whole or in part on these data sets should cite the data source as:* Andreas A, Stoffel T. NREL Solar Radiation Research Laboratory (SRRL): Baseline Measurement System (BMS). National Renewable Energy Laboratory; 1981. Report No.: DA-5500-56488. <http://dx.doi.org/10.5439/1052221>.
- PSNR. Compute peak signal-to-noise ratio (PSNR) between images. MathWorks India; c2021 [accessed 2021 Nov 1]. <https://in.mathworks.com/help/vision/ref/psnr.html>.
- Setiadi DIM. PSNR vs SSIM: imperceptibility quality assessment for image steganography. *Multimed Tools Appl.* 2021;80:8423–8444. <https://doi.org/10.1007/s11042-020-10035-z>.
- Surabhi N. Image compression techniques: a review. *Int J Eng Dev Res.* 2017. <https://www.ijedr.org/papers/IJEDR1701089.pdf>.
- Tabora V. Human vision and digital color perception. *High-Definition Pro*; 2019 Feb 10 [accessed 2021 Nov 1]. <https://medium.com/hd-pro/human-vision-and-digital-color-perception-91db3b19cc7f>.
- Wikipedia.org. Better portable graphics. Wikimedia Corporation; c2021a [accessed 2021 Nov 1]. [https://en.wikipedia.org/wiki/Better\\_Portable\\_Graphics](https://en.wikipedia.org/wiki/Better_Portable_Graphics).
- Wikipedia.org. JPEG. Wikimedia Corporation; c2021b [accessed 2021 Nov 1]. <https://en.wikipedia.org/wiki/JPEG>.

## **Appendix. Maximum File Storage Calculator Program**

---

---

## A.1 Maximum Storage Calculator Description

---

To advance the image compression results to their practical application, a maximum storage calculator program was built. This tool received four user inputs: average file size, number of images to be saved per hour, available storage size, and the required number of days needed for storing images. The program then calculated the number of images that could be taken per day, total number of images that could be stored, the maximum number of images that could be saved per day, how many bytes/day would be required, and finally how many days and years that the storage would populate before registering as “full”.

An example of the program input/output is given in Figs. A-1 and A-2. The Python code generating the results is also shown.

```
Enter average file size (bytes): 256
Number of images you would like to save per hour: 4
Enter available storage (GB): 256
Number of days you require storage for: 365
```

Fig. A-1 Example of the storage calculator inputs

```
You have adequate amount of storage for your specifications per day.
You will have 96 images/day.
Total number you can store is 1,000,000,000 images.
The maximum amount of images that can be saved/day is 2,739,726.
You require 24,576 bytes/day of storage.
Your available storage will last you 10,416,666 days.
```

Fig. A-2 Example of the storage calculator outputs

```

^ ===== ^
# -*- coding: utf-8 -*-
# =====
# Filename:      Storage_Calculator.py
# Author:       Cadet Hailey Goodman
# Last Rev:    21AUG05, HG
#
# PURPOSE:     Provide user with ma images that can be saved per day, how long
#              the storage will last in years and days
#
# INPUT REQUIREMENTS:
#              1. Average file size,
#              2. Number of images to be saved per hour,
#              3. Available storage space (in GB), and
#              4. Number of days that require storage.
#
# OUTPUT:
#              1. Max images that can be saved/day,
#              2. Total number of images you can save on that storage space
#              3. Maximum amount of image that can be saved per day.
#              4. How many bytes/day of storage,
#              5. Length of time storage will last before becoming full.
# =====

#User input avg file size
filesize = input('Enter average file size (bytes): ')
filesize = int(filesize)
#User input number of images saved per day
num = input('Number of images you would like to save per hour: ')
num = int(num)

#User input available storage
storage = input('Enter available storage (GB): ')
storage = int(storage)

#User input number of days required for storage
days = input('Number of days you require storage for: ')
days = int(days)

picsperday = num * 24

# total number of pictures produced for specific time period
totpics = picsperday * days

# total file size for time period

```

```

totfilesize = totpics * filesize

# Max no. of images that can be saved per day
actual = (storage * 1e9) // filesize
maxperday = actual / days

if maxperday >= picsperday:
    bytesperday = picsperday * filesize
    storedays = (storage * 1e9) / bytesperday
    storeyrs = bytesperday / 365
    print('\nYou have adequate amount of storage for your specifications per
day.\n')
    print(' You will have '+ str(picsperday)+ ' images/day.\n')
    print(' Total number you can store is '
+ "{:,}".format(int(actual))
+ ' images.\n')
    print(' The maximum amount of images that can be saved/day is '
+ "{:,}".format(int(maxperday))+ '.\n')
    print(' You require '+ "{:,}".format(int(bytesperday))+ ' bytes/day of
storage.\n')
    print(' Your available storage will last you '
+ "{:,}".format(int(storedays))+ ' days or '+str(storeyrs)+' years.\n')
else:
    print('\nERROR - you have already exceeded the maximum amount of images
that can be stored per day. Please try again.\n ')
    filesize = input('Enter average file size (bytes): ')
    filesize = int(filesize)

    num = input('Number of images you would like to save per hour: ')
    num = int(num)

    storage = input('Enter available storage (GB): ')
    storage = int(storage)

    days = input('Number of days you require storage for: ')
    days = int(days)

    picsperday = num * 24

# total number of pictures produced for specific time period
totpics = picsperday * days

# total file size for time period
totfilesize = totpics * filesize

# Max no. of images that can be saved per day

```

```

actual = (storage * 1e9) // filesize
maxperday = actual / days

if maxperday >= picsperday:
    bytesperday = picsperday * filesize
    storedays = (storage * 1e9) / bytesperday
    years = storedays // 365

    print("\nYou have adequate amount of storage for your specifications per
day.\n')
    print(' You will have '+ str(picsperday)+ ' images/day.\n')
    print(' Total number you can store is '
        + "{:,}".format(int(actual))
        + ' images.\n')
    print(' The maximum amount of images that can be saved/day is '
        + "{:,}".format(int(maxperday))+ '.\n')
    print(' You require '+ "{:,}".format(int(bytesperday))+ ' bytes/day of
storage.\n')
    print(' Your available storage will last you '
        + "{:,}".format(int(years))+ ' years.\n')

else:
    print("\nERROR - you have already exceeded the maximum amount of
images that can be stored per day.')
^ ===== ^
(END OF PROGRAM CODE)

```

## List of Symbols, Abbreviations, and Acronyms

---

AIHPG	Atmospheric Intelligence for Hybrid Power Grid
ARL	Army Research Laboratory
BMP	bitmap
CR	compression ratio
DCT	discrete cosine transform
DEVCOM	US Army Combat Capabilities Development Command
GIF	Graphics Interchange Format
IDC	image detail compression
IRC	image resolution compression
JPEG or JPG	Joint Photographic Experts Group
LT	Local Time
ML	machine learning
NREL	National Renewable Energy Laboratory
PCC	percent cloud cover
PNG	Portable Network Graphics
PSNR	peak signal-to-noise ratio
QL	quality level
RGB	red, green, blue (color channels)
SR	solar radiation
WSI	whole sky imager

1 DEFENSE TECHNICAL  
(PDF) INFORMATION CTR  
DTIC OCA

1 DEVCOM ARL  
(PDF) FCDD RLD DCI  
TECH LIB

1 ATEC  
(PDF) S STARTZ

1 UCF  
(PDF) H GOODMAN

1 MTU  
(PDF) G PARKER

1 C5ISR  
(PDF) M BAILEY

1 GVSC  
(PDF) D RIZZO

12 DEVCOM ARL  
(PDF) FCDD RLC E  
(5 HC) B MCCALL  
T JAMESON  
FCDD RLC ED  
G VAUCHER (5 HC)  
C HOCUT  
R BRICE  
R RANDALL  
M LEE  
M S DARCY  
J RABY  
FCDD RLS RP  
M BERMAN  
B GEIL  
R JANE